Cooperative Manipulation via Internal Force Regulation: A Rigidity Theory Perspective

Christos K. Verginis, *Member, IEEE*, Daniel Zelazo, *Senior Member, IEEE*, and Dimos V. Dimarogonas, *Senior Member, IEEE*

***Abstract*—This article considers the integration of rigid cooperative manipulation with rigidity theory. Motivated by rigid models of cooperative manipulation systems, i.e., where the grasping contacts are rigid, we introduce, first, the notion of bearing and distance rigidity for graph frameworks in SE(3). Next, we associate the nodes of these frameworks to the robotic agents of rigid cooperative manipulation schemes and we express the object-agent internal forces by using the graph rigidity matrix, which encodes the infinitesimal rigid body motions of the system. Moreover, we show that the associated cooperative manipulation grasp matrix is related to the rigidity matrix via a range-nullspace relation, based on which we provide novel results on the relation between the arising interaction and internal forces and, consequently, on the energy-optimal force distribution on a cooperative manipulation system. Finally, simulation results enhance the validity of the theoretical findings.**

***Index Terms*—Bearing rigidity, cooperative manipulation, distance rigidity, infinitesimal rigidity.**

I. Introduction

MULTIROBOT systems have received a considerable amount of attention during the last few decades, due to the advantages they offer with respect to single-robot setups. Example problems include consensus/rendezvous, connectivity maintenance, formation control, and robotic manipulation. In the latter case, multirobot frameworks can yield significant advantages due to the potentially heavy payloads or challenging maneuvers. This work focuses on bridging the fields of cooperative robotic manipulation and robot formation control by associating the interagent interaction forces of the first to interagent geometric relations of the latter.

The goal of robot formation control is to control each robot using local information from neighboring agents so that the entire team forms a desired spatial geometric pattern [1]. A special instance of formation control with numerous applications is *rigid formations*. Two cases of rigid formation control have been widely studied in the literature, namely, *distance rigidity* and *bearing rigidity*. Rigidity theory, a branch of discrete mathematics, explores under what conditions can the geometric pattern of a network be determined given that the length (distance) or bearing of each edge in a network of nodes is fixed. This theory has been applied in distance and bearing formation control and localization problems [2]–[6].

In this article, we introduce the notion of *distance and bearing rigidity*, which studies under what conditions can the geometric pattern of a multiagent system be uniquely determined if both the *distance* and the *bearing* of each edge are fixed. Moreover, we combine the latter with *rigid* cooperative manipulation, i.e., configurations where a number of robots carry an object via rigid contact points. Cooperative manipulation is a special form of constrained dynamical system [7]–[12]. The majority of related works assumes that the robotic agents are attached to the object via *rigid grasps* and, hence, the overall system can be considered as a closed-chain robotic agent. In terms of control design, most works consider decentralized schemes, where there is no communication between the agents, and use impedance and/or force control [13]–[16], possibly with contact force/torque measurements (e.g., [17], [18]). In addition, numerous works consider unknown dynamics/kinematics of the agents and the object and/or external disturbances [19]–[22].

An important property in rigid cooperative manipulation systems that has been studied thoroughly in the related literature is the regulation of internal forces. Internal forces are forces exerted by the agents at the grasping points that do not contribute to the motion of the object. While a certain amount of such forces is required in many cases (e.g., to avoid contact loss in multifingered manipulation), they need to be minimized in order to prevent object damage and unnecessary effort of the agents. Most works in rigid cooperative manipulation assume a certain decomposition of the interaction forces in motion-inducing and internal ones, without explicitly showing that the actual internal forces will be indeed regulated to the desired ones (e.g., [17],

Manuscript received 30 June 2021; revised 26 October 2021; accepted 1 May 2022. Date of publication 10 June 2022; date of current version 17 August 2023. This work was supported in part by H2020 ERC Starting Grant BUCOPHSYS, in part by the European Union's Horizon 2020 Research and Innovation Programme under Grant 731869 (Co4Robots), in part by Swedish Research Council (VR), in part by Knut och Alice Wallenberg Foundation (KAW), and in part by the Swedish Foundation for Strategic Research (SSF). Recommended by Associate Editor M. Prandini.
(Corresponding author: Christos K. Verginis.)

Christos K. Verginis is with the Division of Signals and Systems, Department of Electrical Engineering, Uppsala University, 75237 Uppsala, Sweden (e-mail: christos.verginis@angstrom.uu.se).

Dimos V. Dimarogonas is with the KTH Royal Institute of Technology, 10044 Stockholm, Sweden (e-mail: dimos@kth.se).

Daniel Zelazo is with the Technion-Israel Institute of Technology, Haifa 32000, Israel (e-mail: dzelazo@technion.ac.il).
Digital Object Identifier 10.1109/TCNS.2022.3181724

[18]); [9], [12], [23]–[25] analyze specific load decompositions based on whether they provide internal force-free expressions, whereas [26] is concerned with the cooperative manipulation interaction dynamics. The decompositions in the aforementioned works, however, are based on the interagent distances and do not take into account the actual dynamics of the agents. The latter, as we show in this article, are tightly connected to the internal forces as well as their relation to the total force exerted by the agents. More specifically, the contribution of this article is two-fold. First, we integrate rigid cooperative manipulation with rigidity theory. Motivated by rigid cooperative manipulation systems, where the interagent distances *and* bearings are fixed, we introduce the notion of *distance and bearing rigidity* in the special Euclidean group $\mathsf{SE}(3)$. Based on recent results, we show next that the internal forces in a rigid cooperative manipulation system, consisting of more than two robotic agents, depend on the distance and bearing rigidity matrix, a matrix that encodes the allowed coordinated motions of the multiagent-object system. Moreover, we prove that the cooperative manipulation grasp matrix, which relates the object and agent velocities, is connected via a range-nullspace relation to the rigidity matrix. Second, we rely on the aforementioned findings to provide new results on the internal force-based rigid cooperative manipulation. We derive novel results on the relation between the arising interaction and internal forces in a cooperative manipulation system. This leads to novel conditions on the internal force-free object-agents force distribution and consequently to optimal, in terms of energy resources, cooperative manipulation. Bearing rigidity has been used before in [27] to analyze the properties of virtual closed-loop mechanisms and parallel robots; similarly, our analysis provides new physical insights for the fields of cooperative manipulation and rigidity theory. This article extends our preliminary conference version [28], which tackles optimal cooperative manipulation by regulating the internal forces. That work, however, does not associate cooperative manipulation with rigidity theory or provide *explicit* results on the optimal object-agents force distribution.

The rest of this article is organized as follows. Section II provides notation and necessary background. Section III provides the cooperative manipulation model and Section IV discusses distance and bearing rigidity. The main results of the article are given in Section V, and Section VI discusses features of our analysis. Section VII presents simulation results. Finally, Section VIII concludes this article.

II. Preliminaries

The set of positive integers is denoted by $\mathbb{N}$ and the real n-coordinate space, with $n \in \mathbb{N}$, by $\mathbb{R}^n$. The $n \times n$ identity matrix is denoted by I_n, the n-dimensional zero vector by 0_n, and the $n \times m$ matrix with zero entries by $0_{n\times m}$. We write 0 instead of 0_n when n is clear from the context. The vectors of the canonical basis of $\mathbb{R}^d$ are indicated as $\mathbf{e}_i,\ i \in \{1 \dots d\}$, and they have a one in the $(i \bmod d)$th entry and zeros elsewhere. Given a matrix $A \in \mathbb{R}^{n\times m}$, we use $A^\dagger$ for its Moore–Penrose inverse, and null(A), range(A) for its nullspace and range space, respectively. For a discrete set $\mathcal{N}$, $|\mathcal{N}|$ denotes its cardinality. Given $a, b \in \mathbb{R}^3$, $S(a)$ is the skew-symmetric matrix defined according to $S(a)b = a \times b$. In addition, S^n denotes the $(n+1)$-dimensional sphere and $\mathsf{SO}(3)$, $\mathsf{SE}(3)$ the rotation and special Euclidean group, respectively; $P_r(x) := I_n - \frac{xx^\top}{\|x\|^2}$ projects vector $x \in \mathbb{R}^n$ onto the orthogonal complement of x, i.e., the subspace $\{y \in \mathbb{R}^n : y^\top x = 0\}$. A graph $\mathcal{G}$ is a pair $(\mathcal{N}, \mathcal{E})$, where $\mathcal{N}$ is a finite set of $N = |\mathcal{N}| \in \mathbb{N}$ nodes and $\mathcal{E} \subseteq \mathcal{N} \times \mathcal{N}$ is a finite set of $|\mathcal{E}|$ edges. The complete graph on N nodes is denoted by $\mathcal{K}_N$. All vectors and vector differentiations are expressed with respect to a known inertial reference frame, unless otherwise stated.

We also make use of some properties from linear algebra. 1) For any matrix H, it holds that $H^\dagger = H^\top (HH^\top)^\dagger$ [29, Th. 3.8]. 2) For a matrix $A \in \mathbb{R}^{n\times m}$, and $B := KA$, where $K \in \mathbb{R}^{n\times n}$ is an invertible matrix, it holds that $A^\dagger A = B^\dagger B$. 3) Let $A, B \in \mathbb{R}^{n\times m}$ such that range$(A^\top)$ = null(B). Then, it holds that $A^\dagger A + B^\dagger B = I_m$. 4) For matrices $A, B \in \mathbb{R}^{n\times m}$, A is *left equivalent* (or *row equivalent*) to B if and only if there exists an invertible matrix $P \in \mathbb{R}^{n\times n}$ such that $A = PB$. It then can be shown that A and B are left-equivalent if and only if null(A) = null(B).

Lemma 1 (Gauss' principle [10], [11]): Let an unconstrained system described by the configuration variables $q \in \mathbb{R}^n$ evolve according to $M(q,t)\ddot{q} = Q(q,\dot{q},t)$, where $M \in \mathbb{R}^{n\times n}$ is positive definite. Assume now that the system is subjected to m consistent constraints of the form $A(q,\dot{q},t)\ddot{q} = b(q,\dot{q},t)$. Then, the acceleration $\ddot{q}$ of the constrained system is given by the constrained minimization problem

$$\min_{\ddot{q}} \ [\ddot{q} - \alpha]^\top M(q)[\ddot{q} - \alpha] \quad \text{s.t.} \quad A(q,\dot{q},t)\ddot{q} = b(q,\dot{q},t)$$

where $\alpha := M(q)^{-1}Q(q,\dot{q},t)$ is the acceleration of the unconstrained system.

III. Cooperative Manipulation Modeling

We provide in this section the dynamic modeling of the rigid cooperative manipulation system. A key feature of the model is the grasp matrix, which, as will be clarified, motivates the introduction of the notion of distance and bearing rigidity in the next section and the association between the two.

Consider N robotic agents, indexed by the set $\mathcal{N} := \{1,\dots,N\}$, rigidly grasping an object. We denote by $q_i, \dot{q}_i \in \mathbb{R}^{n_i}$, with $n_i \in \mathbb{N}\ \forall i \in \mathcal{N}$, the generalized joint-space variables and their derivatives of agent i. The overall joint configuration is then $q := [q_1^\top,\dots,q_N^\top]^\top, \dot{q} := [\dot{q}_1^\top,\dots,\dot{q}_N^\top]^\top \in \mathbb{R}^n$, with $n := \sum_{i\in\mathcal{N}} n_i$. In addition, we denote the position and rotation matrix of the ith end-effector by $p_i \in \mathbb{R}^3$ and $R_i \in \mathsf{SO}(3)$, respectively. Similarly, the velocity of the ith end-effector is denoted by $v_i := [\dot{p}_i^\top, \omega_i^\top]^\top$, where $\omega_i \in \mathbb{R}^3$ is the respective angular velocity, and it holds that $v_i = J_i(q_i)\dot{q}_i$, where $J_i : \mathbb{S}_i \to \mathbb{R}^{6\times n_i}$ is the robot Jacobian, and $\mathbb{S}_i := \{q_i \in \mathbb{R}^{n_i} : \dim(\text{null}(J_i(q_i))) = 0\}$ is the set away from kinematic singularities [30], $\forall i \in \mathcal{N}$. Moreover, we denote $x_i := (p_i, R_i) \in \mathsf{SE}(3)$ and $x := (x_1,\dots,x_N) \in \mathsf{SE}(3)^N$. The task-space dynamics of the agents are [30]

$$M(x)\dot{v} + C(x,\dot{x})v + g(x) = u - h \tag{1}$$

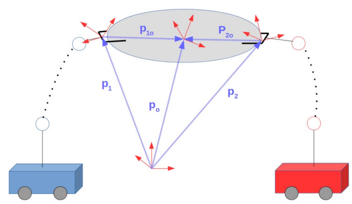

Fig. 1. Two robotic agents rigidly grasping an object.

where $v := [v_1^\top, \ldots, v_N^\top] \in \mathbb{R}^{6N}$, $h := [h_1^\top, \ldots, h_N^\top]^\top$, $u := [u_1^\top, \ldots, u_N^\top]^\top$, $g := [g_1^\top, \ldots, g_N^\top]^\top \in \mathbb{R}^{6N}$; the terms $M_i : \mathbb{S}_i \to \mathbb{R}^{6\times 6}, C_i : \mathbb{S}_i \times \mathbb{R}^6 \to \mathbb{R}^{6\times 6}, g_i : \mathbb{S}_i \to \mathbb{R}^6$ are their positive definite inertia, Coriolis, and gravity terms, respectively, which are well-defined when $q_i \in \mathbb{S}_i$, $i \in \mathcal{N}$; $h_i \in \mathbb{R}^6$ are the forces between the object and the agents, and $u_i \in \mathbb{R}^6$ the task-space inputs $\forall i \in \mathcal{N}$.

Regarding the object, we denote by $x_O := (p_O, R_O) \in \mathsf{SE}(3)$ and $v_O := [\dot{p}_O^\top, \omega_O^\top]^\top \in \mathbb{R}^{12}$ the pose and generalized velocity of the object's center of mass, respectively. We consider the following second-order dynamics, which can be derived based on the Newton–Euler formulation:

$$\dot{R}_O = S(\omega_O)R_O \tag{2a}$$

$$M_O(x_O)\dot{v}_O + C_O(x_O, \dot{x}_O)v_O + g_O(x_O) = h_O \tag{2b}$$

where $M_O : \mathsf{SE}(3) \to \mathbb{R}^{6\times 6}$ is the positive definite inertia matrix, $C_O : \mathsf{SE}(3) \times \mathbb{R}^6 \to \mathbb{R}^{6\times 6}$ is the Coriolis matrix, $g_O : \mathsf{SE}(3) \to \mathbb{R}^6$ is the gravity vector, and $h_O \in \mathbb{R}^6$ is the vector of generalized forces acting on the object's center of mass.

In view of Fig. 1 and the grasping rigidity, one obtains [19]

$$v_i = J_{O_i}(x_i)v_O \; \forall i \in \mathcal{N} \tag{3}$$

where $J_{O_i} : \mathsf{SE}(3) \to \mathbb{R}^{6\times 6}$ is the object-to-agent Jacobian matrix, with

$$J_{O_i}(x_i) = \begin{bmatrix} I_3 & -S(p_{iO}) \\ 0_{3\times 3} & I_3 \end{bmatrix} \tag{4}$$

and $p_{iO} := p_i - p_O, \forall i \in \mathcal{N}$; J_{O_i} is always full-rank, due to the rigidity of the grasping contacts. The grasp matrix is formed by stacking $J_{O_i}^\top$ as

$$G(x) := \left[J_{O_1}(x_1)^\top, \ldots, J_{O_N}(x_N)^\top\right] \in \mathbb{R}^{6\times 6N} \tag{5}$$

and has full-column rank due to the rigidity of the grasping contacts; (3) can now be written in stack vector form as

$$v = G(x)^\top v_O. \tag{6}$$

The kineto-statics duality [30] along with the grasp rigidity suggests that the force h_O acting on the object's center of mass and the generalized forces $h_i, i \in \mathcal{N}$, exerted by the agents at the grasping points, are related through

$$h_O = G(x)h. \tag{7}$$

By using (1), (2), and (7), we obtain the coupled dynamics

$$M_{\mathsf{c}}(\bar{x})\dot{v}_O + C_{\mathsf{c}}(\bar{x}, \dot{\bar{x}})v_O + g_{\mathsf{c}}(\bar{x}) = G(x)u \tag{8}$$

where $M_{\mathsf{c}} := M_O + GMG^\top$, $C_{\mathsf{c}} := C_O + GCG^\top + GM\dot{G}^\top$, $g_{\mathsf{c}} := g_O + Gg$, $\bar{x}$ is the coupled state $\bar{x} := [x^\top, x_O^\top]^\top \in \mathsf{SE}(3)^{N+1}$, and we have omitted the arguments for brevity. The interaction forces h between the object and the agents can be decoupled into motion-induced and internal forces

$$h = h_{\text{m}} + h_{\text{int}}. \tag{9}$$

The internal forces h_{int} are squeezing forces that the agents exert to the object and belong to the nullspace of $G(x)$ [i.e., $G(x)h_{\text{int}} = 0$]. Intuitively, when $h = h_{\text{int}}$, it holds that $G(x)(u - M\dot{v} - Cv - g) = 0$ and the object moves according to $h_O = M_O\dot{v}_O + C_Ov_O + g_O = 0$. Hence, h_{int} does not contribute to the object's motion and results in internal stresses that might damage it. An analytic expression for h and h_{int} is given in Section V.

Note from (6) that the agent velocities v belong to the range space of $G(x)^\top$. Therefore, since $G(x)$ is a matrix that encodes rigidity constraints, this motivates the association of $G(x)$ to the *rigidity matrix* used in formation rigidity theory, and of the rigid cooperative manipulation scheme to a multiagent rigid formation scheme. To this end, we introduce next in Section IV the notion of distance and bearing rigidity. In Section V-A, we connect the latter with the cooperative manipulation system (8), and in Section V-B, we use this connection to derive new results on cooperative manipulation free from internal forces. We argue that the association of rigid cooperative manipulation with rigidity theory, which has not been considered before, provides new physical insights in the intersection of the two fields (illustrated in Theorem 1 of Section V). It also paves the way for drawing novel links that could help solve problems of one by leveraging the rich literature of the other.

IV. Distance and Bearing Rigidity in $\mathsf{SE}(3)$

We begin by recalling that the range space of the grasp matrix $G(x)^T$ corresponds to the rigid body translations and rotations of the system. While G appears naturally in the context of dynamic modeling of rigid bodies, it is also indirectly related to the notion of structural rigidity in discrete geometry.

In the classical structural rigidity theory, one considers a collection of rigid bars connected by joints allowing free rotations around the joint axis (*bar-and-joint* frameworks). One is then interested in understanding what are the allowable motions of the framework, i.e., those motions that preserve the lengths of the bars and their connections to the joints. The so-called *trivial motions* for these frameworks are precisely the rigid body translations and rotations of the system. For some frameworks, there may be additional motions, known as *flexes*, that also preserve the constraints. This is captured by the notion of *infinitesimal motions* of the framework and is characterized by the *rigidity matrix* of the framework [31].

Since, in a rigid cooperative manipulation system, the relative distances and bearings among the agents and the object are *fixed*, we naturally consider frameworks that encode both the lengths of bars and pose of the joints, leading to a *distance- and bearing*-type framework. This relates notions from distance rigidity, and recent works in bearing rigidity for frameworks embedded in

$\mathsf{SE}(2)$ and $\mathsf{SE}(3)$ [32], [33]. In this direction, we introduce the concept of distance and bearing rigidity (abbreviated as D&B rigidity). For this work, we focus on the notion of infinitesimal rigidity for D&B frameworks. We first formally define a D&B framework in $\mathsf{SE}(3)$.

Definition 1: A framework in $\mathsf{SE}(3)$ is a triple $(\mathcal{G}, p_\mathcal{G}, R_\mathcal{G})$, where $\mathcal{G} := (\mathcal{N}, \mathcal{E})$ is a graph, $p_\mathcal{G} : \mathcal{N} \to \mathbb{R}^3$ is a function mapping each node to a position in $\mathbb{R}^3$, and $R_\mathcal{G} : \mathcal{N} \to \mathrm{SO}(3)$ is a function associating each node with an orientation element of SO(3) (both with respect to an inertial frame).

In this work, we employ the special orthogonal group (rotation matrices) $\{R \in \mathbb{R}^{3\times 3} : R^\top R = I_3, \det(R) = 1\}$ to express the orientation of the agents. Moreover, we use the shorthand notation $p_i := p_\mathcal{G}(i), R_i := R_\mathcal{G}(i), p := [p_1^\top, \dots, p_N^\top]^\top \in \mathbb{R}^{3N}$, $R := (R_1, \dots, R_N) \in \mathsf{SO}(3)^N$, $x_i := (p_i, R_i) \in \mathsf{SE}(3)$, and $x := (x_1, \dots, x_N) \in \mathsf{SE}(3)^N$.

The distances and bearings in a framework can be summarized through the following *$\mathsf{SE}(3)$ D&B rigidity function*, $\gamma_\mathcal{G}$, that encodes the rigidity constraints in the framework. Consider a directed graph $\mathcal{G} = (\mathcal{N}, \mathcal{E})$, where $\mathcal{E} \subseteq \{(i, j) \in \mathcal{N}^2 : i \neq j\}$, as well as $\mathcal{E}_u := \{(i, j) \in \mathcal{E} : i < j\} \subseteq \mathcal{E}$. Then, $\gamma_\mathcal{G}$ can be formed by the distance and bearing functions $\gamma_{e,d} : \mathbb{R}^3 \times \mathbb{R}^3 \to \mathbb{R}_{\geq 0}$, $\gamma_{e,b} : \mathsf{SE}(3)^2 \to \mathsf{S}^2$, with

$$\gamma_{e,d}(p_i, p_j) := \frac{1}{2}\|p_i - p_j\|^2 \; \forall e = (i, j) \in \mathcal{E}_u \tag{10a}$$

$$\gamma_{e,b}(x_i, x_j) := R_i^\top \frac{p_j - p_i}{\|p_i - p_j\|} \; \forall e = (i, j) \in \mathcal{E} \tag{10b}$$

which encodes the distance $\|p_i - p_j\|$ between two agents as well as the local bearing vector $R_i^\top \frac{p_j - p_i}{\|p_i - p_j\|}$, expressed in the frame of agent i. Now $\gamma_\mathcal{G}$ is formed by stacking the aforementioned distance and bearing functions, i.e., $\gamma_\mathcal{G} : \mathsf{SE}(3)^N \to \mathbb{R}^{|\mathcal{E}_u|} \times \mathsf{S}^{2|\mathcal{E}|}$, with

$$\gamma_\mathcal{G} := \begin{bmatrix} \gamma_d(p) \\ \gamma_b(x) \end{bmatrix} := \left[\gamma_{1,d}, \dots, \gamma_{|\mathcal{E}_u|,d}, \gamma_{1,b}^\top, \dots, \gamma_{|\mathcal{E}|,b}^\top\right]^\top. \tag{11}$$

We have introduced the edge set $\mathcal{E}_u$ for the symmetric distance functions $\gamma_{(i,j),d} = \gamma_{(j,i),d}$ in order to avoid redundancy in the rows of $\gamma_\mathcal{G}$. Note that the aforementioned expressions for $\gamma_{e,d}$, $\gamma_{e,b}$ are not unique and other choices that capture the rigidity constraints can also be made. We also mention our slight abuse of notation, where the index k in $\gamma_{k,d}$ and $\gamma_{k,b}$ refers to a labeled edge in $\mathcal{E}_u$ and $\mathcal{E}$.

In this work, we are interested in the set of D&B *infinitesimal* motions of a framework in $\mathsf{SE}(3)$. These can be thought as perturbations to a framework in $\mathsf{SE}(3)$ that leave $\gamma_\mathcal{G}$ unchanged. This set is characterized by the nullspace of the matrix appearing in the rate-of-change of $\gamma_\mathcal{G}$ under the kinematic equations associated with rotational motion in $\mathsf{SE}(3)$ [33]. That is, the nullspace of the matrix $\nabla_{(p,R)}\gamma_\mathcal{G}$, termed the $\mathsf{SE}(3)$-D&B *rigidity matrix* $\mathcal{R}_\mathcal{G} : \mathsf{SE}(3)^N \to \mathbb{R}^{(|\mathcal{E}_u| + 3|\mathcal{E}|)\times 6N} := \nabla_{(p,R)}\gamma_\mathcal{G}$, i.e.,

$$\mathcal{R}_\mathcal{G}(x) = \begin{bmatrix} \frac{\partial \gamma_{1,d}}{\partial p_1} & \frac{\partial \gamma_{1,d}}{\partial R_1} & \cdots & \frac{\partial \gamma_{1,d}}{\partial p_N} & \frac{\partial \gamma_{1,d}}{\partial R_N} \\ \vdots & & \ddots & & \vdots \\ \frac{\partial \gamma_{|\mathcal{E}_u|,d}}{\partial p_1} & \frac{\partial \gamma_{|\mathcal{E}_u|,d}}{\partial R_1} & \cdots & \frac{\partial \gamma_{|\mathcal{E}_u|,d}}{\partial p_N} & \frac{\partial \gamma_{|\mathcal{E}_u|,d}}{\partial R_N} \\ \frac{\partial \gamma_{1,b}}{\partial p_1} & \frac{\partial \gamma_{1,b}}{\partial R_1} & \cdots & \frac{\partial \gamma_{1,b}}{\partial p_N} & \frac{\partial \gamma_{1,b}}{\partial R_N} \\ \vdots & & \ddots & & \vdots \\ \frac{\partial \gamma_{|\mathcal{E}|,b}}{\partial p_1} & \frac{\partial \gamma_{|\mathcal{E}|,b}}{\partial R_1} & \cdots & \frac{\partial \gamma_{|\mathcal{E}|,b}}{\partial p_N} & \frac{\partial \gamma_{|\mathcal{E}|,b}}{\partial R_N} \end{bmatrix} \tag{12}$$

with

$$\frac{\partial \gamma_{e,d}}{\partial x_i} = \begin{bmatrix} \frac{\partial \gamma_{e,d}}{\partial p_i} & \frac{\partial \gamma_{e,d}}{\partial R_i} \end{bmatrix} = \begin{bmatrix} (p_i - p_j)^\top & 0_{1\times 3} \end{bmatrix}$$

$$\frac{\partial \gamma_{e,d}}{\partial x_j} = \begin{bmatrix} \frac{\partial \gamma_{e,d}}{\partial p_j} & \frac{\partial \gamma_{e,d}}{\partial R_j} \end{bmatrix} = \begin{bmatrix} (p_j - p_i)^\top & 0_{1\times 3} \end{bmatrix}$$

$$\frac{\partial \gamma_{e,b}}{\partial x_i} = \begin{bmatrix} \frac{\partial \gamma_{e,b}}{\partial p_i} & \frac{\partial \gamma_{e,b}}{\partial R_i} \end{bmatrix} = \begin{bmatrix} -\frac{P_r(\gamma_{e,b})}{\|p_j - p_i\|} R_i^\top & S(\gamma_{e,b}) R_i^\top \end{bmatrix}$$

$$\frac{\partial \gamma_{e,b}}{\partial x_j} = \begin{bmatrix} \frac{\partial \gamma_{e,b}}{\partial p_j} & \frac{\partial \gamma_{e,b}}{\partial R_j} \end{bmatrix} = \begin{bmatrix} \frac{P_r(\gamma_{e,b})}{\|p_j - p_i\|} R_i^\top & 0_{3\times 3} \end{bmatrix}.$$

The projection operator $P_r(\cdot)$ [5] is defined as in Section II. Infinitesimal motions, therefore, are motions $x(t)$ produced by velocities $v(t)$ that lie in the nullspace of $\mathcal{R}_\mathcal{G}$, for which it holds that $\dot{\gamma}_\mathcal{G} = \mathcal{R}_\mathcal{G}(x(t))v(t) = 0$, where $v := [\dot{p}_1^\top, \omega_1^\top, \dots, \dot{p}_N^\top, \omega_N^\top]^\top$, as defined in Section III. The infinitesimal motions therefore depend on the number of motion degrees of freedom the entire framework possesses. This directly relates to the structure of the underlying graph. Motions that preserve the distances and bearings of the framework for *any* underlying graph are called *D&B trivial motions*. This leads to the definition of *infinitesimal rigidity*.

Definition 2: A framework $(\mathcal{G}, p_\mathcal{G}, R_\mathcal{G})$ is D&B infinitesimally rigid in $\mathsf{SE}(3)$ if every D&B infinitesimal motion is a D&B trivial motion.

We now aim to identify what the trivial motions of a D&B framework are, and to determine conditions for a framework to be infinitesimally rigid based on properties of $\mathcal{R}_\mathcal{G}$. Before we proceed, we note that the D&B rigidity function in $\mathsf{SE}(3)$ can be seen as a superposition of the rigidity functions associated with the classic distance rigidity theory [31] and the $\mathsf{SE}(3)$ bearing rigidity theory [32]. In particular, we note that $\mathcal{R}_{\mathcal{G},d} : \mathbb{R}^{3N} \to \mathbb{R}^{|\mathcal{E}_u|\times 3N} := \nabla_p\gamma_d$ is the well-studied (distance) rigidity matrix, while $\mathcal{R}_{\mathcal{G},b} : \mathsf{SE}^{3N} \to \mathbb{R}^{3|\mathcal{E}|\times 6N} := \nabla_{(p,R)}\gamma_{\mathcal{G},b}$ is the $\mathsf{SE}(3)$ bearing rigidity matrix. Note that $\mathcal{R}_{\mathcal{G},d}$ is associated with the framework $(\mathcal{G}, p_\mathcal{G})$, which is the projection of $(\mathcal{G}, p_\mathcal{G}, R_\mathcal{G})$ to $\mathbb{R}^3$. With an appropriate permutation, P_R, of the columns of $\mathcal{R}_\mathcal{G}$, we have that

$$\widetilde{\mathcal{R}}_\mathcal{G} := \mathcal{R}_\mathcal{G} P_R$$
$$= \begin{bmatrix} \frac{\partial \gamma_{1,d}}{\partial p_1} & \cdots & \frac{\partial \gamma_{1,d}}{\partial p_N} & \frac{\partial \gamma_{1,d}}{\partial R_1} & \cdots & \frac{\partial \gamma_{1,d}}{\partial R_N} \\ \vdots & & \ddots & & \vdots & \\ \frac{\partial \gamma_{M_\mathcal{G},d}}{\partial p_1} & \cdots & \frac{\partial \gamma_{M_\mathcal{G},d}}{\partial p_N} & \frac{\partial \gamma_{M_\mathcal{G},d}}{\partial R_1} & \cdots & \frac{\partial \gamma_{M_\mathcal{G},d}}{\partial R_N} \\ \frac{\partial \gamma_{1,b}}{\partial p_1} & \cdots & \frac{\partial \gamma_{1,b}}{\partial p_N} & \frac{\partial \gamma_{1,b}}{\partial R_1} & \cdots & \frac{\partial \gamma_{1,b}}{\partial R_N} \\ \vdots & & \ddots & & \vdots & \\ \frac{\partial \gamma_{M_\mathcal{G},b}}{\partial p_1} & \cdots & \frac{\partial \gamma_{M_\mathcal{G},b}}{\partial p_N} & \frac{\partial \gamma_{M_\mathcal{G},b}}{\partial R_1} & \cdots & \frac{\partial \gamma_{M_\mathcal{G},b}}{\partial R_N} \end{bmatrix} \quad (13)$$

which is equal to

$$\widetilde{\mathcal{R}}_\mathcal{G} = \begin{bmatrix} \begin{bmatrix} \mathcal{R}_{\mathcal{G},d} & 0_{|\mathcal{E}_u|\times 3N} \end{bmatrix} \\ \mathcal{R}_{\mathcal{G},b} \end{bmatrix} =: \begin{bmatrix} \bar{\mathcal{R}}_{\mathcal{G},d} \\ \mathcal{R}_{\mathcal{G},b} \end{bmatrix}.$$

The nullspace of $\widetilde{\mathcal{R}}_\mathcal{G}$, therefore, is the intersection of the nullspaces of $\bar{\mathcal{R}}_{\mathcal{G},d}$ and $\mathcal{R}_{\mathcal{G},b}$.

With the above interpretation, we can now understand the trivial motions to be the intersection of trivial motions associated to distance rigidity with those associated to $\mathsf{SE}(3)$ bearing rigidity. In particular, let

$$\mathcal{S}_d := \text{span}\left\{1_N \otimes I_3, \mathcal{L}^{\circlearrowright}_{\mathbb{R}^3}(\mathcal{G})\right\}$$

denote the trivial motions associated to a distance framework [31]. That is, $1_N \otimes I_3$ represents translations of the entire framework, and $\mathcal{L}^{\circlearrowright}_{\mathbb{R}^3}(\mathcal{G})$ is the rotational subspace induced by the graph $\mathcal{G}$ in $\mathbb{R}^3$, i.e.,

$$\mathcal{L}^{\circlearrowright}_{\mathbb{R}^3}(\mathcal{G}) = \text{span}\left\{(I_N \otimes S(\mathbf{e}_h))\, p_\mathcal{G}, h = 1,2,3\right\}.$$

These motions can be produced by the *linear* velocities of the agents. It is known that $\mathcal{S}_d \subseteq \text{null}(\mathcal{R}_{\mathcal{G},d})$ for any underlying graph $\mathcal{G}$ [31]. For the matrix $\bar{\mathcal{R}}_{\mathcal{G},d}$, we can define the corresponding set

$$\bar{S}_d := \text{span}\left\{\begin{bmatrix} 1_N \otimes I_3 \\ \star \end{bmatrix}, \begin{bmatrix} \mathcal{L}^{\circlearrowright}_{\mathbb{R}^3}(\mathcal{G}) \\ \star \end{bmatrix}\right\} \subseteq \text{null}(\bar{\mathcal{R}}_{\mathcal{G},d}).$$

Note that the distance rigidity does not explicitly depend on the orientation of the nodes when expressed as a point in $\mathsf{SE}(3)$. This accounts for the free $\star$ entry in the subspace $\bar{S}_d$ corresponding to the rotations. Thus, the set of trivial motions in $\mathbb{R}^3$ can be seen as the projection of $\bar{S}_d$ in $\mathbb{R}^3$.

Similarly, for an $\mathsf{SE}(3)$ bearing framework one can define the subspace [32]

$$\mathcal{S}_b := \text{span}\left\{\begin{bmatrix} 1_N \otimes I_3 \\ 0_{3N\times 3}, \end{bmatrix}, \begin{bmatrix} p_\mathcal{G} \\ 0_{3N}, \end{bmatrix}, \mathcal{L}^{\circlearrowright}_{\mathsf{SE}(3)}(\mathcal{G})\right\}$$

where the vector $[p_\mathcal{G}^T, 0_{3N}^T]^T$ represents a scaling of the framework. The space $\mathcal{L}^{\circlearrowright}_{\mathsf{SE}(3)}(\mathcal{G})$ is the rotational subspace induced by $\mathcal{G}$, in $\mathsf{SE}(3)$,

$$\mathcal{L}^{\circlearrowright}_{\mathsf{SE}(3)}(\mathcal{G}) = \text{span}\left\{\begin{bmatrix} (I_N \otimes S(\mathbf{e}_h))\, p_\mathcal{G} \\ 1_N \otimes \mathbf{e}_h \end{bmatrix}, h = 1,2,3\right\}. \quad (14)$$

It is also known that $\mathcal{S}_b \subseteq \text{null}(\mathcal{R}_{\mathcal{G},b})$. Thus, $\mathcal{S}_b$ describes the trivial motions of an $\mathsf{SE}(3)$ bearing framework [32]. The above discussion leads to the following result.

Proposition 1: The trivial motions of a D&B framework are characterized by the set

$$\mathcal{S}_{db} := \bar{\mathcal{S}}_d \cap \mathcal{S}_b = \text{span}\left\{\begin{bmatrix} 1_N \otimes I_3 \\ 0_{3N\times 3} \end{bmatrix}, \mathcal{L}^{\circlearrowright}_{\mathsf{SE}(3)}(\mathcal{G})\right\}.$$

Furthermore, it follows that $\mathcal{S}_{db} \subseteq \text{null}(\widetilde{\mathcal{R}}_\mathcal{G})$.

Having characterized the trivial motions, it now follows from Definition 2 that for infinitesimal rigidity, we require that $\text{null}(\widetilde{\mathcal{R}}_\mathcal{G}) = \mathcal{S}_{db}$. This is summarized as follows.

Proposition 2: The framework $(\mathcal{G}, p_\mathcal{G}, R_\mathcal{G})$ is D&B infinitesimally rigid in $\mathsf{SE}(3)$ if and only if

$$\text{null}(\widetilde{\mathcal{R}}_\mathcal{G}) = \text{null}(\bar{\mathcal{R}}_{\mathcal{G},d}) \cap \text{null}(\mathcal{R}_{\mathcal{G},b})$$
$$= \text{span}\left\{\begin{bmatrix} 1_N \otimes I_3 \\ 0_{3N\times 3}, \end{bmatrix}, \mathcal{L}^{\circlearrowright}_{\mathsf{SE}(3)}(\mathcal{G})\right\} = \mathcal{S}_{db}. \quad (15)$$

Equivalently, the D&B framework is infinitesimally rigid in $\mathsf{SE}(3)$ if and only if

$$\text{rank}(\widetilde{\mathcal{R}}_\mathcal{G}) = \dim(\widetilde{\mathcal{R}}_\mathcal{G}) - \dim(\text{null}(\widetilde{\mathcal{R}}_\mathcal{G})) = 6N - 6. \quad (16)$$

Hence, all the motions produced by the nullspace of $\widetilde{\mathcal{R}}_\mathcal{G}$ for an infinitesimally rigid framework must correspond to trivial motions, i.e., translations and coordinated rotations.

Moreover, given (13), it follows that $(\mathcal{G}, p_\mathcal{G}, R_\mathcal{G})$ is D&B infinitesimally rigid in $\mathsf{SE}(3)$ if and only if

$$\text{null}(\mathcal{R}_\mathcal{G}) = \{x = P_R y \in \mathsf{SE}(3)^N : y \in \text{null}(\widetilde{\mathcal{R}}_\mathcal{G})\} \quad (17)$$

i.e., the nullspace of $\mathcal{R}_\mathcal{G}$ consists of the vectors of $\text{null}(\widetilde{\mathcal{R}}_\mathcal{G})$ whose elements are permutated by P_R.

It is worth noting that the aforementioned results are not valid if the rigidity matrix loses rank, i.e., $\text{rank}(\mathcal{R}_\mathcal{G}) < \max\{\text{rank}(\mathcal{R}_\mathcal{G}(x)), x \in \mathsf{SE}(3)\}$. These are degenerate cases that correspond, for example, to when all agents are aligned along a direction $\mathbf{v} \in \mathsf{S}^2$. In particular, frameworks with $N = 2$ nodes are also degenerate by this definition. For more discussion on these cases, the reader is referred to [33]. As a last remark, we observe that frameworks over the complete graph, $(\mathcal{K}_N, p_{\mathcal{K}_N}, R_{\mathcal{K}_N})$, are (except for the degenerate configurations) infinitesimally rigid. That is, $\text{rank}(\widetilde{\mathcal{R}}_{\mathcal{K}_N}) = 6N - 6$. This result follows from the literature on distance- and $\mathsf{SE}(3)$-rigidity theory [31], [32]. This leads to the following corollary.

Corollary 1: Consider the D&B frameworks $(\mathcal{G}, p_\mathcal{G}, R_\mathcal{G})$ and $(\mathcal{K}_N, p_\mathcal{G}, R_\mathcal{G})$ for nondegenrate configurations $(p_\mathcal{G}, R_\mathcal{G})$. Then, $(\mathcal{G}, p_\mathcal{G}, R_\mathcal{G})$ is D&B infinitesimally rigid if and only if $\text{rank}(\widetilde{\mathcal{R}}_\mathcal{G}) = \text{rank}(\widetilde{\mathcal{R}}_{\mathcal{K}_N}) = 6N - 6$.

In the next section, we use the aforementioned results to link the D&B rigidity matrix of a complete graph to the internal forces from (9).

V. Main Results

In cooperative manipulation schemes, the most energy-efficient way of transporting an object is to exploit the full potential of the cooperating robotic agents, i.e., each agent does not exert less effort at the expense of other agents, which might then potentially exert more effort than necessary. For instance, consider a rigid cooperative manipulation scheme, with only one agent (a leader) working toward bringing the object to a desired location, whereas the other agents have zero inputs. Since the grasps are rigid, if the leader is equipped with sufficiently powerful actuators, it will achieve the task by "dragging" the rest of the agents, compensating for their dynamics, and creating non-negligible internal forces. In such cases, when the cooperative manipulation system is rigid (i.e., the grasps are considered to be rigid), the optimal strategy of transporting an object is achieved by regulating the internal forces to zero. Therefore, from a control perspective, the goal of a rigid cooperative manipulation system is to design a control protocol that achieves a desired cooperative manipulation task, while guaranteeing that the internal forces remain zero.

This section provides the main results of this work. We first give, in Section V-A, a closed-form expression for the internal forces of the coupled object-agents system, by connecting them with the D&B rigidity matrix introduced in Section IV. Next, we use these results in Section V-B to provide a novel relation between the arising interaction and internal forces; we further give conditions on the agent force distribution for cooperative manipulation free from internal forces.

A. Internal Forces Based on the D&B Rigidity Matrix

In this section, we provide a closed-form expression for the internal forces of the coupled object-agents system and link them to the D&B rigidity matrix notion introduced in Section IV. In particular, we consider that the robotic agents form a graph that will be defined in the sequel. Note that, due to the rigidity of the grasping points, the forces exerted by an agent influence, not only the object, but all the other agents as well. Hence, since there exists interaction among all the pairs of agents, we model their connection as a complete graph, as explicitly described below. Moreover, as will be clarified later, the rigidity matrix of this graph encodes the constraints among the agents, imposed by the rigidity of the grasping points, and plays an important role in the expression of the internal forces.

Let the robotic agents form a framework $(\mathcal{G}, p_{\mathcal{G}}, R_{\mathcal{G}})$ in $\mathsf{SE}(3)$, where $\mathcal{G} := (\mathcal{N}, \mathcal{E})$ is the complete graph, i.e., $\mathcal{E} = \{(i,j) \in \mathcal{N}^2 : i \neq j\}$, and $p_{\mathcal{G}} := [p_1^\top, \dots, p_N^\top]^\top$, $R_{\mathcal{G}} := (R_1, \dots, R_N)$. Consider also the undirected part $\mathcal{E}_u = \{(i,j) \in \mathcal{E} : i < j\}$ of $\mathcal{E}$, as also described in Section IV. Since the graph is complete, we conclude that $|\mathcal{E}| = N(N-1)$ and $|\mathcal{E}_u| = \frac{N(N-1)}{2}$. Consider now the rigidity functions $\gamma_{e,d} : \mathbb{R}^3 \times \mathbb{R}^3 \to \mathbb{R}_{\geq 0}$, $\forall e \in \bar{\mathcal{E}}_u$ and $\gamma_{e,b} : \mathsf{SE}(3)^2 \to \mathsf{S}^2$, $\forall e \in \mathcal{E}$, as given in (10), as well as the stack vector $\gamma_{\mathcal{G}} : \mathsf{SE}(3)^N \to \mathbb{R}^{\frac{N(N-1)}{2}} \times \mathsf{S}^{2N(N-1)}$ as given in (11). The rigidity constraints of the framework are encoded in the constraint $\gamma_{\mathcal{G}} = \text{const}$. Since the rigidity of the framework stems from the rigidity of the grasping points, these constraints encode also the rigidity constraints of the object-agent cooperative manipulation. By differentiating twice $\gamma_{\mathcal{G}} = \text{const.}$, one obtains

$$\mathcal{R}_{\mathcal{G}}(x)\dot{v} = -\dot{\mathcal{R}}_{\mathcal{G}}(x)v \qquad (18)$$

where $\mathcal{R}_{\mathcal{G}} : \mathsf{SE}(3)^N \to \mathbb{R}^{\frac{7N(N-1)}{2} \times (6N)}$ is the rigidity matrix associated to $\mathcal{G}$ and has the form (12). Note that (18) is derived from $\gamma_{\mathcal{G}}$, which corresponds to the distance and bearing constraints for a complete graph; hence, using Corollary 1, $\gamma_{\mathcal{G}}$ encodes rigid body motions (coordinated translations and rotations of the system). Therefore, by assuming that the agents satisfy the constraint $\dot{\gamma}_{\mathcal{G}} = \mathcal{R}_{\mathcal{G}}v = 0$ initially,[1] we conclude that the motion of the cooperative object-agents manipulation system that is enforced by (18) corresponds to rigid body motions (coordinated translations and rotations of the system). Hence, since $\mathcal{G}$ is complete, the analysis of Section IV dictates that these motions are the infinitesimal motions of the framework and are the ones produced by the nullspace of $\mathcal{R}_{\mathcal{G}}(x)$. We note that the rigid body motions *can* be produced by the nullspace of the rigidity matrix of other graph topologies as well (except for the complete one). Nevertheless, as explained above, the complete graph topology draws motivation from the physics of the cooperative manipulation system, where all agents indeed influence the object as well as each other via their exerted forces.

After giving the rigidity constraints in the cooperative manipulation system, we are now ready to derive the expressions for the internal forces, h_{int}, in terms of the aforementioned rigidity matrix. We follow the same methodology as in [9]. Since we are concerned with the internal forces, consider, without loss of generality, that $h_O = h_{\text{m}} = 0 \Leftrightarrow h = h_{\text{int}}$, i.e., the agents produce only internal forces, without inducing object acceleration. Then, the agent dynamics are

$$M(x)\dot{v} + C(x,\dot{x})v + g(x) = u - h_{\text{int}}. \qquad (19)$$

We use Gauss' principle [10], [11] (see Lemma 1) to derive a closed form expression for h_{int}. Let the *unconstrained* system of the robotic agents be $M(x)\alpha(x,\dot{x}) := u - C(x,\dot{x})v - g(x)$, where α is the unconstrained acceleration, i.e., the acceleration the system would have if the agents did not grasp the object. According to Gauss's principle [10], the actual acceleration $\dot{v}$ of the system is the closest one to α, while satisfying the rigidity constraints. More rigorously, and as stated in Lemma 1, $\dot{v}$ is the solution of the constrained minimization problem

$$\begin{aligned} \min \quad & [\dot{v} - \alpha(x,\dot{x})]^\top M(x) [\dot{v} - \alpha(x,\dot{x})] \\ \text{s.t.} \quad & \mathcal{R}_{\mathcal{G}}(x)\dot{v} = -\dot{\mathcal{R}}_{\mathcal{G}}(x)v. \end{aligned}$$

The solution to this problem is obtained by using the Karush–Kuhn–Tucker conditions [34] and has a closed-form expression. It can be shown that it satisfies

$$M\dot{v} = M\alpha - \mathcal{R}_{\mathcal{G}}^\top \left(\mathcal{R}_{\mathcal{G}} M^{-1} \mathcal{R}_{\mathcal{G}}^\top\right)^\dagger \left(\dot{\mathcal{R}}_{\mathcal{G}}v + \mathcal{R}_{\mathcal{G}}\alpha\right)$$

which is consistent with the one in [10],

$$M\dot{v} = M\alpha - M^{\frac{1}{2}} \left(\mathcal{R}_{\mathcal{G}} M^{-\frac{1}{2}}\right)^\dagger \left(\dot{\mathcal{R}}_{\mathcal{G}}v + \mathcal{R}_{\mathcal{G}}\alpha\right)$$

since it holds that $\mathcal{R}_{\mathcal{G}}^\top(\mathcal{R}_{\mathcal{G}} M^{-1} \mathcal{R}_{\mathcal{G}}^\top)^\dagger = M^{\frac{1}{2}}(\mathcal{R}_{\mathcal{G}} M^{-\frac{1}{2}})^\dagger$. Indeed, according to property 1) of Section II, it holds that $H^\dagger = H^\top(HH^\top)^\dagger$, for any $H \in \mathbb{R}^{x \times y}$. Then, the aforementioned equality is obtained by setting $H = \mathcal{R}_{\mathcal{G}} M^{-\frac{1}{2}}$.

[1] Otherwise, the constraint $\mathcal{R}_{\mathcal{G}}v = 0$ can be appended in (18).

Therefore, the internal forces have the form

$$h_{\text{int}} = \mathcal{R}_{\mathcal{G}}^{\top}\left(\mathcal{R}_{\mathcal{G}}M^{-1}\mathcal{R}_{\mathcal{G}}^{\top}\right)^{\dagger}\left(\dot{\mathcal{R}}_{\mathcal{G}}v + \mathcal{R}_{\mathcal{G}}\alpha\right) \tag{20a}$$

$$= M^{\frac{1}{2}}\left(\mathcal{R}_{\mathcal{G}}M^{-\frac{1}{2}}\right)^{\dagger}\left(\dot{\mathcal{R}}_{\mathcal{G}}v + \mathcal{R}_{\mathcal{G}}\alpha\right) \tag{20b}$$

and one concludes that when the unconstrained motion of the system does not satisfy the constraints (i.e., when $\dot{\mathcal{R}}_{\mathcal{G}}v \neq -\mathcal{R}_{\mathcal{G}}\alpha$), then the actual accelerations of the system are modified in a manner directly proportional to the extent to which these constraints are violated. Moreover, it is evident from the aforementioned expression that the internal forces depend not only on the relative distances $p_i - p_j$, but also on the closed-loop dynamics and the inertia of the unconstrained system (see the dependence on α_{int} and B). Therefore, given a desired force h_{d} to be applied to the object, an internal force-free distribution to agent forces $h_{i,\text{d}}$ at the grasping points cannot be independent of the system dynamics. We stress that the derived expression concerns the internal forces produced exclusively by the redundancy of the multirobot system (excluding, for instance, potential internal forces needed to keep the object from falling due to gravity, which would also arise in a single manipulation task). By following a similar procedure and including the object in the multiagent graph, one can arrive to similar results for the interaction forces h as well.

Note that, as dictated in Section IV, the rigidity matrix $\mathcal{R}_{\mathcal{G}}$ is not unique, since different choices of $\gamma_{\mathcal{G}}$ that encode the rigidity constraints can be made. Hence, one might think that different expressions of $\mathcal{R}_{\mathcal{G}}$ will result in different rigidity constraints of the form (18) and hence different internal forces—which is unreasonable. Therefore, in order to show the consistency of (20), we prove next in Proposition 3 that this is not the case, by using the fact that all different expressions of the rigidity matrix $\mathcal{R}_{\mathcal{G}}$ have the same nullspace (the coordinated translations and rotations of the framework).

Proposition 3: Let $\mathcal{R}_{\mathcal{G},1}$ and $\mathcal{R}_{\mathcal{G},2}$ such that $\text{null}\left(\mathcal{R}_{\mathcal{G},1}\right) = \text{null}\left(\mathcal{R}_{\mathcal{G},2}\right)$ and let

$$h_{\text{int},i} := M^{\frac{1}{2}}\left(\mathcal{R}_{\mathcal{G},i}M^{-\frac{1}{2}}\right)^{\dagger}\left(\dot{\mathcal{R}}_{\mathcal{G},i}v + \mathcal{R}_{\mathcal{G},i}\alpha_{\text{int}}\right), \quad \forall i \in \{1,2\}.$$

Then, $h_{\text{int},1} = h_{\text{int},2}$.

Proof: The poses and velocities in the terms $\dot{\mathcal{R}}_{\mathcal{G},i}v$ are the actual ones resulting from the coupled system dynamics and hence they respect the rigidity constraints imposed by $R_{\mathcal{G},i}\dot{v} = -\dot{\mathcal{R}}_{\mathcal{G},i}v$, for $i \in \{1,2\}$. Therefore, exploiting the positive definiteness of M, we need to prove that $(\mathcal{R}_{\mathcal{G},1}M^{-\frac{1}{2}})^{\dagger}\mathcal{R}_{\mathcal{G},1} = (\mathcal{R}_{\mathcal{G},2}M^{-\frac{1}{2}})^{\dagger}\mathcal{R}_{\mathcal{G},2}$. According to property 4) of Section II, since $\mathcal{R}_{\mathcal{G},1}$ and $\mathcal{R}_{\mathcal{G},2}$ have the same nullspace, they are left equivalent matrices and there exists an invertible matrix P such that $\mathcal{R}_{\mathcal{G},1} = P\mathcal{R}_{\mathcal{G},2}$. Hence, by further using property 2) of Section II, it holds that

$$\left(\mathcal{R}_{\mathcal{G},2}M^{-\frac{1}{2}}\right)^{\dagger}\mathcal{R}_{\mathcal{G},2} - \left(\mathcal{R}_{\mathcal{G},1}M^{-\frac{1}{2}}\right)^{\dagger}\mathcal{R}_{\mathcal{G},1}$$

$$= \left[(\mathcal{R}_{\mathcal{G},2}M^{-\frac{1}{2}})^{\dagger}\mathcal{R}_{\mathcal{G},2}M^{-\frac{1}{2}} - (P\mathcal{R}_{\mathcal{G},2}M^{-\frac{1}{2}})^{\dagger}P\mathcal{R}_{\mathcal{G},2}M^{-\frac{1}{2}}\right]M^{\frac{1}{2}}$$

which is equal to 0. ■

Additionally, by following its proof, one can conclude that Proposition 3 can be extended to account for different graphs $\mathcal{G}$ and $\mathcal{G}'$ satisfying (18).

Next, we note that (20) leads to the following Lemma.

Lemma 2: The cooperative manipulation system is free of internal forces, i.e., $h_{\text{int}} = 0_{6N}$, if and only if

$$\dot{\mathcal{R}}_{\mathcal{G}}v + \mathcal{R}_{\mathcal{G}}M^{-1}\left(u - C\dot{v} - g\right) \in \text{null}\left(\mathcal{R}_{\mathcal{G}}^{\top}\right).$$

Proof: In view of (20), $\dot{\mathcal{R}}_{\mathcal{G}}v + \mathcal{R}_{\mathcal{G}}\alpha_{\text{int}} = \dot{\mathcal{R}}_{\mathcal{G}}v + \mathcal{R}_{\mathcal{G}}M^{-1}$ $(u - C\dot{v} - g)$ must belong to null $\left(M^{\frac{1}{2}}\left(\mathcal{R}_{\mathcal{G}}M^{-\frac{1}{2}}\right)^{\dagger}\right)$ in order to avoid internal forces. The latter, however, is identical to null $\left(\mathcal{R}_{\mathcal{G}}^{\top}\right)$, since it holds that null $\left(\mathcal{R}_{\mathcal{G}}M^{-1/2}\right)^{\dagger} =$ null $\left(M^{-\frac{1}{2}}\mathcal{R}_{\mathcal{G}}^{\top}\right)$ and M is positive definite. ■

As mentioned before, the most energy-efficient way of transporting an object in a cooperative manipulation scheme is by minimizing the arising internal forces. In the next section, we derive a new relation between the interaction and internal forces as well as novel sufficient and necessary conditions on the agent force distribution for the provable regulation of the internal forces to zero, according to (20). We further show its application in a standard inverse-dynamics control law that guarantees trajectory tracking by the object's center of mass.

B. Cooperative Manipulation Via Internal Force Regulation

In this section, we use the results of Section V-A to derive a new relation between the interaction and internal forces h and h_{int}, respectively. Moreover, we derive novel sufficient and necessary conditions on the agent force distribution for the provable regulation of the internal forces to zero, according to (20), and we show its application in a standard inverse-dynamics control law that guarantees trajectory tracking of the object's center of mass. This is based on the following main theorem, which links the complete agent graph rigidity matrix $\mathcal{R}_{\mathcal{G}}$ to the grasp matrix G.

Theorem 1: Let N robotic agents, with configuration $x = (p, R) \in \mathsf{SE}(3)^N$, rigidly grasping an object and associated with a grasp matrix $G(x)$, as in (5). Let also the agents be modeled by a framework on the complete graph $(\mathcal{K}_N, p_{\mathcal{K}_N}, R_{\mathcal{K}_N}) = (\mathcal{K}_N, p, R)$ in $\mathsf{SE}(3)$, which is associated with a rigidity matrix $\mathcal{R}_{\mathcal{K}_N}$. Let also x be such that $\text{rank}(\mathcal{R}_{\mathcal{K}_N}(x)) = \max_{y \in \mathsf{SE}(3)^N}\{\text{rank}(\mathcal{R}_{\mathcal{K}_N}(y))\}$. Then,

$$\text{null}(G(x)) = \text{range}\left(\mathcal{R}_{\mathcal{K}_N}(x)^{\top}\right). \tag{21}$$

Proof: Since $\mathcal{R}_{\mathcal{K}_N}$ corresponds to the complete graph and $\text{rank}(\mathcal{R}_{\mathcal{K}_N}(x)) = \max_{y \in \mathsf{SE}(3)^N}\{\text{rank}(\mathcal{R}_{\mathcal{K}_N}(y))\}$, the framework $(\mathcal{K}_N, p, R)$ is infinitesimally rigid. Hence, the nullspace of $\mathcal{R}_{\mathcal{K}_N}$ consists only of the infinitesimal motions of the framework, i.e., coordinated translations and rotations, as defined in Proposition 1. In particular, in view of (17), Proposition 2, and (14), one concludes that $\text{null}(\mathcal{R}_{\mathcal{K}_N})$ is the linear span of $1_N \otimes \begin{bmatrix} I_3 \\ 0_{3\times 3} \end{bmatrix}$ and the vector space $[\chi_1^{\top}, \ldots, \chi_N^{\top}]^{\top} \in \mathsf{SE}(3)^N$, with $\chi_i := [\chi_{i,p}^\top, \chi_{i,R}^\top]^\top \in \mathsf{SE}(3)$, satisfying

$$\chi_{i,p} - \chi_{j,p} = -S(p_i - p_j)\chi_{i,R} \tag{22a}$$

$$\chi_{i,R} = \chi_{j,R} \tag{22b}$$

where $p_i := p_{\mathcal{K}_N}(i)$, $p_j := p_{\mathcal{K}_N}(j)$ $\forall i,j \in \mathcal{N}$, with $i \neq j$. In view of (6), one obtains $v = G(x)^\top v_O$. Note that the first three columns of $G^\top$ form the space $1_N \otimes \begin{bmatrix} I_3 \\ 0_{3\times 3}\end{bmatrix}$, whereas its last three columns span the aforementioned rotation vector space. Indeed, for any $\dot{p}_O, \omega_O \in \mathbb{R}^6$, the range of these columns is

$$\left[-\dot{p}_O^\top S(p_{1O})^\top, \omega_O^\top, \ldots, -\dot{p}_O^\top S(p_{NO})^\top, \omega_O^\top\right]^\top$$

for which it is straightforward to verify that (22) holds. Hence, $\text{null}(\mathcal{R}_{\mathcal{K}_N}) = \text{range}(G^\top)$, which implies (21). ■

We note that, in degenerate cases (i.e., when $\mathcal{R}_\mathcal{G}$ loses rank, as explained in Section IV), $\text{null}(\mathcal{R}_\mathcal{G})$ contains more motions than the trivial coordinated translations and rotations, i.e., $\text{range}(G^\top) \subset \text{null}(\mathcal{R}_\mathcal{G})$. Therefore, (21) is replaced by $\text{range}(\mathcal{R}_\mathcal{G}^\top) \subset \text{null}(G)$.

Since the internal forces belong to $\text{null}(G)$, one concludes that they are composed of all the vectors z for which there exists a y such that $z = \mathcal{R}_\mathcal{G}^\top y$. This can also be verified by inspecting (20b); one can prove that $\text{range}(M^{\frac{1}{2}}(\mathcal{R}_\mathcal{G} M^{-\frac{1}{2}})^\dagger) = \text{range}(\mathcal{R}_\mathcal{G}^\top)$. The aforementioned result provides significant insight regarding the control of the motion of the coupled cooperative manipulation system. In particular, by using (20b) and Theorem 1, we provide next new conditions on the agent force distribution for provable avoidance of internal forces. We first derive a novel relation between the agent forces h and the internal forces h_{int}.

In many related works, h is decomposed as

$$h = G^* G h + (I - G^* G) h \tag{23}$$

where G^* is a right inverse of G. The term G^*Gh is a projection of h on the range space of $G^\top$, whereas the term $(I - G^*G)h$ is a projection of h on the null space of G. A common choice is the Moore–Penrose inverse $G^* = G^\dagger = G^\top(GG^\top)^{-1}$. This specific choice yields the vector $G^*Gh = G^\dagger G h \in \text{range}(G^\top)$ that is closest to h, i.e., $\|h - G^\dagger G h\| \leq \|h - y\|$, $\forall y \in \text{range}(G^\top)$. However, as the next theorem states, if the second term of (23) must equal h_{int}, as defined in (20), G^* must equal $MG^\top(GMG^\top)^{-1}$.

Theorem 2: Consider N robotic agents rigidly grasping an object with coupled dynamics (8). Let $h \in \mathbb{R}^{6N}$ be the stacked vector of agent forces exerted at the grasping points. Then, the agent forces h and the internal forces h_{int} are related as

$$h_{\text{int}} = \left(I_{6N} - MG^\top(GMG^\top)^{-1}G\right) h.$$

In order to prove Theorem 2, we first need the following result.

Proposition 4: Consider the grasp and rigidity matrices G, $\mathcal{R}_\mathcal{G}$, of (5), (12), respectively. Then, it holds that

$$MG^\top\left(GMG^\top\right)^{-1}G + M^{\frac{1}{2}}\left(\mathcal{R}_\mathcal{G} M^{-\frac{1}{2}}\right)^\dagger \mathcal{R}_\mathcal{G} M^{-1} = I. \tag{24}$$

Proof: Let $A := \mathcal{R}_\mathcal{G} M^{-\frac{1}{2}}$ and $B := GM^{\frac{1}{2}}$. Then, $\text{range}(A^\top) = \text{null}(B)$. Indeed, according to Theorem 1, it holds that if $z = \mathcal{R}_\mathcal{G}^\top y$, for some $y \in \mathbb{R}^6$, then $Gz = 0_6$. By multiplying by $M^{-\frac{1}{2}}$, we obtain $M^{-\frac{1}{2}} z = M^{-\frac{1}{2}}\mathcal{R}_\mathcal{G}^\top y$, which implies that $\hat{z} := M^{-\frac{1}{2}} z \in \text{range}((\mathcal{R}_\mathcal{G} M^{\frac{1}{2}})^\top)$. It also holds that $B\hat{z} = GM^{\frac{1}{2}}\hat{z} = Gz = 0_6$, and hence $\hat{z} \in \text{null}(B)$. Therefore, by using properties 1) and 3) of Section II and the fact that $GMG^\top$ is invertible, we conclude that

$$\left(GM^{\frac{1}{2}}\right)^\dagger GM^{\frac{1}{2}} + \left(\mathcal{R}_\mathcal{G} M^{-\frac{1}{2}}\right)^\dagger \mathcal{R}_\mathcal{G} M^{-\frac{1}{2}} = I$$

$$\Leftrightarrow M^{\frac{1}{2}} G^\top \left(GMG^\top\right)^\dagger GM^{\frac{1}{2}} + \left(\mathcal{R}_\mathcal{G} M^{-\frac{1}{2}}\right)^\dagger \mathcal{R}_\mathcal{G} M^{-\frac{1}{2}} = I$$

and by left and right multiplication by $M^{\frac{1}{2}}$ and $M^{-\frac{1}{2}}$, respectively, the result follows. ■

Moreover, for the proof of Theorem 2, we need the following expression, which is derived from (6), (1), (2), and (7).

$$h = \left(M^{-1} + G^\top M_O^{-1} G\right)^{-1}\Big[M^{-1}(u - g - Cv) - \dot{G}^\top v_O + G^\top M_O^{-1}\left(C_O v_O + g_O\right)\Big]. \tag{25}$$

Proof of Theorem 2: We first show that

$$\left[I - MG^\top\left(GMG^\top\right)^{-1} G\right]\left(M^{-1} + G^\top M_O^{-1} G\right)^{-1} = M^{\frac{1}{2}}\left(\mathcal{R}_\mathcal{G} M^{-\frac{1}{2}}\right)^\dagger \mathcal{R}_\mathcal{G}.$$

Indeed, since $(M^{-1} + G^\top M_O^{-1} G)^{-1}$ has full rank, it suffices to show that

$$I - MG^\top\left(GMG^\top\right)^{-1} G = M^{\frac{1}{2}}\left(\mathcal{R}_\mathcal{G} M^{-\frac{1}{2}}\right)^\dagger \mathcal{R}_\mathcal{G}\left(M^{-1} + G^\top M_O^{-1} G\right)$$

which can be concluded from the fact that $\mathcal{R}_\mathcal{G} G^\top = 0$ (due to Theorem 1) and Proposition 4. Therefore, in view of (25), it holds that

$$\begin{aligned}&\left(I - MG^\top\left(GMG^\top\right)^{-1} G\right) h \\ &= \left[I - MG^\top\left(GMG^\top\right)^{-1} G\right]\left(M^{-1} + G^\top M_O^{-1} G\right)^{-1}\Big[-\dot{G}^\top v_O \\ &\quad + M^{-1}(u - g - Cv) + G^\top M_O^{-1}\left(C_O v_O + g_O\right)\Big] \\ &= M^{\frac{1}{2}}\left(\mathcal{R}_\mathcal{G} M^{-\frac{1}{2}}\right)^\dagger \mathcal{R}_\mathcal{G}\Big[M^{-1}(u - g - Cv) \\ &\quad + G^\top M_O^{-1}\left(C_O v_O + g_O\right) - \dot{G}^\top v_O\Big]\end{aligned}$$

which, in view of the facts that $\mathcal{R}_\mathcal{G} G^\top = 0$, and hence $-\mathcal{R}_\mathcal{G}\dot{G}^\top = \dot{\mathcal{R}}_\mathcal{G} G^\top$, as well as $G^\top v_O = v$, becomes

$$M^{\frac{1}{2}}(\mathcal{R}_\mathcal{G} M^{-\frac{1}{2}})^\dagger[\dot{\mathcal{R}}_\mathcal{G} v + \mathcal{R}_\mathcal{G} M^{-1}(u - g - Cv)] = h_{\text{int}}.$$

■

Based on Theorem 2, we provide next new results on the internal force-free (optimal) distribution of a force to the agents.

Theorem 3: Consider N robotic agents rigidly grasping an object with coupled dynamics (8). Let a desired force to be applied to the object $h_{O,\text{d}} \in \mathbb{R}^6$, which is distributed to the agents' desired forces as $h_\text{d} = G^* h_{O,\text{d}}$, and where G^* is a right inverse of G, i.e., $GG^* = I_6$. Then, it holds that

$$h_\text{int} = 0 \Leftrightarrow G^* = MG^\top (GMG^\top)^{-1}.$$

Proof: First, it is easily verified that G^* is a pseudo-inverse of G [29]. Next, according to Theorem 2, the derivation of h_d that yields zero internal forces can be formulated as a quadratic minimization problem

$$\text{QP}: \quad \min_{h_\text{d}} \quad \|h_\text{int}\|^2 = h_\text{d}^\top H h_\text{d} \quad \text{s.t.} \quad G h_\text{d} = h_{O,\text{d}} \tag{26}$$

where $H := (I_{6N} - MG^\top (GMG^\top)^{-1} G)^\top (I_{6N} - MG^\top (GMG^\top)^{-1} G)$. Note that the choice $G^* = MG^\top (GMG^\top)^{-1} h_{O,\text{d}}$ is a minimizer of QP, since $GG^* = I_6$, and $HG^* h_{O,\text{d}} = 0_{6N}$, and therefore sufficiency is proved.

In order to prove necessity, we prove next that G^* is a strict minimizer, i.e., there is no other right inverse of G that is a solution to of QP. Note first that $G \in \mathbb{R}^{6 \times 6N}$ has full row rank, which implies that the dimension of its nullspace is $6N - 6$. Let $Z := [z_1, \ldots, z_{6N-6}] \in \mathbb{R}^{6N \times (6N-6)}$ be the matrix formed by the vectors $z_1, \ldots, z_{6N-6} \in \mathbb{R}^{6N}$ that span the nullspace of G. It follows that $\text{rank}(Z) = 6N - 6$ and $GZ = 0_{6 \times 6N-6}$. Let now the matrix $H' := Z^\top H Z \in \mathbb{R}^{(6N-6)\times(6N-6)}$. Since $GZ = 0_{6\times(6N-6)} \Rightarrow Z^\top G^\top = 0_{(6N-6)\times 6}$, it follows that $H' = Z^\top Z$. Hence, $\text{rank}(H') = \text{rank}(Z) = 6N - 6$, which implies that H' is positive definite. Therefore, according to [35, Th. 1.1], QP has a strong minimizer. ■

The aforementioned theorem provides novel necessary and sufficient conditions for provable minimization of internal forces in a cooperative manipulation scheme. As discussed before, this is crucial for achieving energy-optimal cooperative manipulation, where the agents do not have to "waste" control input and hence energy resources that do not contribute to object motion. Related works that focus on deriving internal force-free distributions G^*, e.g., [9], [12], [23]–[25], are solely based on the interagent distances, neglecting the actual dynamics of the agents and the object. The expressions (20), however, give new insight on the topic and suggest that the dynamic terms of the system play a significant role in the arising internal forces, as also indicated by Corollary 2. This is further exploited by Theorem 3 to derive a right-inverse that depends on the inertia of the system. Note also that, as mentioned before and explained in [9], the internal forces depend on the acceleration of the robotic agents and hence the incorporation of M in G^* is something to be expected.

The forces h, however, are not the actual control input of the robotic agents, and hence we cannot simply set $h = h_\text{d} = MG^\top (GMG^\top)^{-1} G h_{O,\text{d}}$ for a given $h_{O,\text{d}}$. Therefore, we design next a standard inverse-dynamics control algorithm controller that guarantees tracking of a desired trajectory by the object center of mass while provably achieving regulation of the internal forces to zero. Provable force regulation is also done in [8], requiring however the constraints matrix ($\mathcal{R}_\mathcal{G}$ in our case) to have positive singular values.

C. Control Design

Let a desired position trajectory for the object center of mass be $p_\text{d} : \mathbb{R}_{\geq 0} \to \mathbb{R}^3$, and $e_p := p_O - p_\text{d}$. Let also a desired object orientation be expressed in terms of a desired rotation matrix $R_\text{d} : \mathbb{R}_{\geq 0} \to \mathsf{SO}(3)$, with $\dot{R}_\text{d} = S(\omega_\text{d}) R_\text{d}$, where $\omega_\text{d} : \mathbb{R}_{\geq 0} \to \mathbb{R}^3$ is the desired angular velocity. Then, an orientation error metric is [36] $e_O := \frac{1}{2}\text{tr}(I_3 - R_\text{d}^\top R_O) \in [0, 2]$, which, after differentiation and by using (2a) and properties of skew-symmetric matrices, becomes [36]

$$\dot{e}_O = \frac{1}{2} e_R^\top R_O^\top (\omega_O - \omega_\text{d}) \tag{27}$$

where $e_R := S^{-1}(R_\text{d}^\top R_O - R_O^\top R_\text{d}) \in \mathbb{R}^3$. The equilibrium $e_R = 0$ corresponds to $e_O = 0$, implying $\text{tr}(R_\text{d}^\top R_O) = 3$ and $R_O = R_\text{d}$, as well as to $e_O = 2$, implying $\text{tr}(R_\text{d}^\top R_O) = -1$ and $R_O \neq R_\text{d}$ [36]. The second case represents an undesired equilibrium, where the desired and the actual orientation differ by 180 degrees. This issue is caused by topological obstructions on $\mathsf{SO}(3)$ and it has been proven that no continuous controller can achieve *global* stabilization [37]. We design next a control protocol that guarantees internal force-free convergence of e_p, e_O, while guaranteeing that $e_O(t) < 2, \forall t \in \mathbb{R}_{\geq 0}$, provided that the right inverse $G^* = MG^\top (GMG^\top)^{-1}$ is used.

Corollary 2: Consider N robotic agents rigidly grasping an object, as described in Section III, with coupled dynamics (8). Let a desired trajectory be defined by $p_\text{d} : \mathbb{R}_{\geq 0} \to \mathbb{R}^3$, $R_\text{d} : \mathbb{R}_{\geq 0} \to \mathsf{SO}(3)$, $\dot{p}_\text{d}, \omega_\text{d} \in \mathbb{R}^3$, and assume that $e_O(0) < 2$. Consider the control law

$$u = g + \left(CG^\top + M\dot{G}^\top\right) v_O + G^*\left(g_O + C_O v_O\right) + \left(MG^\top + G^* M_O\right)\left(\dot{v}_\text{d} - K_d e_v - K_p e_x\right) \tag{28}$$

where $e_v := v_O - v_\text{d}$, $v_\text{d} := [\dot{p}_\text{d}^\top, \omega_\text{d}^\top]^\top \in \mathbb{R}^6$, $e_x := [e_p^\top, \frac{1}{2(2-e_O)^2} e_R^\top R_O^\top]^\top$, $K_p := \text{diag}\{K_{p_1}, k_{p_2} I_3\}$, where $K_{p_1} \in \mathbb{R}^{3\times 3}, K_d \in \mathbb{R}^{6\times 6}$ are positive definite matrices, and $k_{p_2} \in \mathbb{R}_{>0}$ is a positive constant. Then, the solution of the closed-loop coupled system satisfies the following:

1) $e_O(t) < 2, \forall t \in \mathbb{R}_{\geq 0}$.
2) $\lim_{t\to\infty}(p_O(t) - p_\text{d}(t)) = 0_3, \quad \lim_{t\to\infty} R_\text{d}(t)^\top R_O(t) = I_3$.
3) It holds that $h_\text{int}(t) = 0 \Leftrightarrow G^* = MG^\top (GMG^\top)^{-1}$.

Proof: 1) By substituting (28) in (8) and using $GG^* = I$ we obtain, in view of (8) and the positive definiteness of $\widetilde{M}$ that $\widetilde{M}(\bar{x})(\dot{e}_v + K_d e_v + K_p e_x) = 0$, implying

$$\dot{e}_v = -K_d e_v - K_p e_x. \tag{29}$$

Consider now the function $V := \frac{1}{2} e_p^\top K_{p_1} e_p + \frac{k_{p_2}}{2-e_O} + \frac{1}{2} e_v^\top e_v$, for which it holds $V(0) < \infty$, since $e_O(0) < 2$. By differentiating V, and using (27) and (29), one obtains $\dot{V} = -e_v^\top K_d e_v \leq 0$. Hence, it holds that $V(t) \leq V(0) < \infty$, which implies that $\frac{k_{p_2}}{2-e_O(t)}$ is bounded and consequently $e_O(t) < 2$.

2) Since $V(t) \leq V(0) < \infty$, the errors e_p, e_v are bounded, which, given the boundedness of the desired trajectories p_d, R_d and their derivatives, implies the boundedness of the control law u. Hence, it can be proved that $\ddot{V}$ is bounded which implies

the uniform continuity of $\dot{V}$. Therefore, according to Barbalat's lemma ([38], Lemma 8.2), we deduce that $\lim_{t\to\infty}\dot{V}(t)=0 \Rightarrow \lim_{t\to\infty} e_v(t)=0_6$. Since $e_x(t)$ is also bounded, it can be proved by using the same arguments that $\lim_{t\to\infty}\dot{e}_v(t)=0_6$ and hence (29) implies that $\lim_{t\to\infty} e_x(t)=0_6$.

3) Let the desired object force be

$$h_{O,\mathrm{d}} = C_O v_O + g_O + M_O \alpha_\mathrm{d} \tag{30}$$

where $\alpha_\mathrm{d} := \dot{v}_\mathrm{d} - K_d e_v - K_p e_x$. In view of Theorem 3, it suffices to prove $h = h_\mathrm{d} = G^* h_{O,\mathrm{d}}$. By substituting (28) in (25) and canceling terms, we obtain

$$h = \left(M^{-1} + G^\top M_O^{-1} G\right)^{-1} \Big[M^{-1} G^* h_{O,\mathrm{d}} + G^\top \alpha_\mathrm{d} + G^\top M_O^{-1}\left(C_O v_O + g_O\right)\Big].$$

Next, we add and subtract the term $G^\top M_O^{-1} G G^* h_{O,\mathrm{d}}$ as

$$h = \left(M^{-1} + G^\top M_O^{-1} G\right)^{-1}\left(M^{-1} + G^\top M_O^{-1} G\right) G^* h_{O,\mathrm{d}} + \left(M^{-1} + G^\top M_O^{-1} G\right)^{-1}\Big[G^\top M_O^{-1}\Big(M_O \alpha_\mathrm{d} + C_O v_O + g_O - G^\top M_O h_{O,\mathrm{d}}\Big)\Big]$$

which, in view of (30), becomes $h = G^* h_{O,\mathrm{d}}$. Completion of the proof follows by invoking Theorem 3. ■

In case it is required to achieve a *desired* internal force $h_{\mathrm{int,d}}$, one can add in (28) a term of the form described next.

Corollary 3: Let $h_{\mathrm{int,d}} \in \mathrm{null}(G)$ be a desired internal force to be achieved. Then, adding the extra term $u_{\mathrm{int,d}} = (I_{6N} - MG^\top(GMG^\top)^{-1}G)h_{\mathrm{int,d}}$ in (28) achieves $h_{\mathrm{int}} = h_{\mathrm{int,d}}$.

Proof of Corollary 3: Since $h_{\mathrm{int,d}} \in \mathrm{null}(G) = \mathrm{range}(\mathcal{R}_\mathcal{G}^\top)$, it holds that $M^{-\frac{1}{2}} h_{\mathrm{int,d}} \in \mathrm{range}(M^{-\frac{1}{2}}\mathcal{R}_\mathcal{G}^\top) = \mathrm{range}(\mathcal{R}_\mathcal{G} M^{-\frac{1}{2}})^\dagger$. Therefore, it holds that

$$\begin{aligned}&\left(\mathcal{R}_\mathcal{G} M^{-\frac{1}{2}}\right)^\dagger \mathcal{R}_\mathcal{G} M^{-1} h_{\mathrm{int,d}} \\ &= \left(\mathcal{R}_\mathcal{G} M^{-\frac{1}{2}}\right)^\dagger \mathcal{R}_\mathcal{G} M^{-\frac{1}{2}}\left(M^{-\frac{1}{2}} h_{\mathrm{int,d}}\right) \\ &= M^{-\frac{1}{2}} h_{\mathrm{int,d}}.\end{aligned} \tag{31}$$

Hence, (20b) yields the resulting internal forces

$$\begin{aligned} h_{\mathrm{int}} &= M^{\frac{1}{2}}\left(\mathcal{R}_\mathcal{G} M^{-\frac{1}{2}}\right)^\dagger \mathcal{R}_\mathcal{G} M^{-1} \times \left(I - MG^\top\left(GMG^\top\right)^{-1} G\right) h_{\mathrm{int,d}} \\ &= M^{\frac{1}{2}}\left(\mathcal{R}_\mathcal{G} M^{-\frac{1}{2}}\right)^\dagger \mathcal{R}_\mathcal{G} M^{-1} h_{\mathrm{int,d}} \\ &= M^{\frac{1}{2}} M^{-\frac{1}{2}} h_{\mathrm{int,d}} = h_{\mathrm{int,d}}\end{aligned}$$

where we have used (31) and the fact that $\mathcal{R}_\mathcal{G} G^\top = 0$. ■

VI. Discussion

We briefly comment now on some of the features of the aforementioned analysis.

First, we note that the aforementioned results, spanning from Theorem 1 to Corollary 3, still hold if the rigidity matrix $\mathcal{R}_\mathcal{G}$ is replaced by any constraint matrix $\mathcal{A}$ satisfying $\mathcal{A}v = 0$ and (18), not necessarily related to rigidity theory (see, e.g., (10) of [28]). However, the connection between cooperative manipulation and rigidity theory could, through the insight provided by Theorem 1, pave the way for drawing novel links that could help solve problems in the two fields. For instance, one could use rigidity-theory results toward the localization of robotic agents [5], or object-agent contact maintenance via means of rigidity maintenance for non-rigid grasping contacts. Reversely, the association of cooperative manipulation and rigidity theory could help use cooperative-manipulation tools to tackle issues in formations of rigid graphs. For instance, the results on cooperative manipulation free from internal forces could be used to prevent local minima in decentralized formation control of rigid graphs through Theorem 1.

Second, note that $G^\star = MG^\top(GMG^\top)^{-1}$ induces an *implicit* and natural load-sharing scheme via the incorporation of M. More specifically, note that the force distribution to the robotic agents via $G^* h_{O,\mathrm{d}}$ yields for each agent $M_i J_{O_i}(\sum_{i\in\mathcal{N}} J_{O_i}^\top M_i J_{O_i})^{-1}$, $\forall i \in \mathcal{N}$. Hence, larger values of M_i will produce larger inputs for agent i, implying that agents with larger inertia characteristics will take on a larger share of the object load. Note that this is also a *desired* load-sharing scheme, since larger dynamic values usually imply more powerful robotic agents. Previous works (e.g., [17]) used load-sharing coefficients, without relating the resulting force distribution with the arising internal forces.

Third, note that the employed controller requires knowledge of the agent and object dynamics. In case of dynamic parameter uncertainty, standard adaptive control schemes that attempt to estimate potential uncertainties in the model (e.g., [19], [22]) would intrinsically create internal forces, since the dynamics of the system would not be accurately compensated. The same holds for schemes that employ force/torque sensors that provide the respective measurements at the grasp points (e.g., [17], [18]) in periodic time instants. Since the interaction forces depend explicitly on the control input, such measurements will unavoidably correspond to the interaction forces of the previous time instants due to causality reasons, creating thus small disturbances in the dynamic model.

Finally, note that the aforementioned results do not hold in degenerate cases where the rigidity matrix loses rank (see Section IV). In such cases, $\mathrm{null}(\mathcal{R}_\mathcal{G})$ contains more motions than the trivial ones (coordinated translations and rotations), and hence the constraints (18) are not consistent with the motion of the cooperative manipulation system, leading to an inaccurate expression in (20). In these cases, one can employ the constraints' matrix used in [28] [see (10)], whose nullspace always coincides with $\mathrm{range}(G^\top)$.

VII. Simulation Results

This section provides simulation results using four identical UR5 robotic manipulators in the realistic dynamic environment V-REP [39]. The agents are rigidly grasping an object of 40 kg, as shown in Fig. 2. In order to verify the findings of the previous sections, we apply the controller (28) to achieve tracking of a desired trajectory by the object's center of mass. We simulate

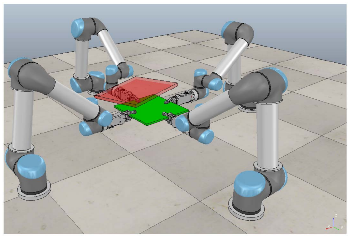

Fig. 2. Four UR5 robotic arms rigidly grasping an object. The red counterpart represents a desired object pose at $t = 0$.

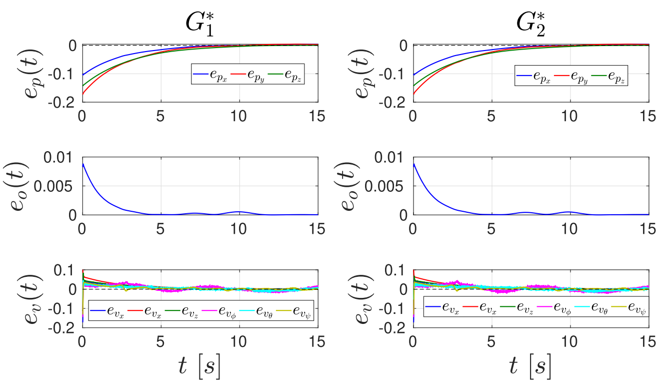

Fig. 3. Error metrics $e_p(t)$, $e_O(t)$, $e_v(t)$, respectively, top to bottom, for the two choices G_1^* and G_2^* and $t \in [0, 15]$ s.

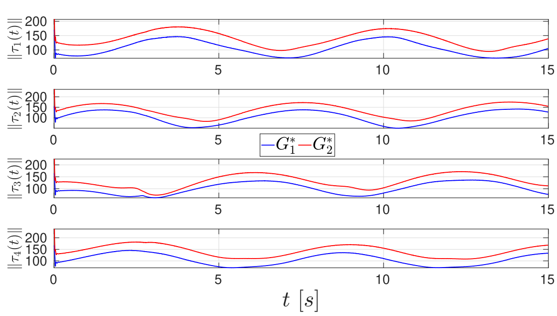

Fig. 4. Norms of the resulting control inputs, $\|\tau_i(t)\|$ for G_1^* (with blue) and G_2^* (with red), $\forall i \in \{1, \dots, 4\}$, and $t \in [0, 15]$ s.

the closed-loop system for two cases of G^*, namely the proposed one $G_1^* = MG^\top(GMG^\top)^{-1}$ as well as the more standard choice $G_2^* = G^\top(GG^\top)^{-1}$, showing the validity of Corollaries 2 and 3.

The initial pose of the object is set as $p_O(0) = [-0.225, -0.612, 0.161]^\top$, $\eta_O(0) = [0, 0, 0]^\top$ and the desired trajectory as $p_{\text{d}}(t) = p_O(0) + [0.2 \sin(w_p dt + \varphi_{\text{d}}), 0.2 \cos(w_p t + \varphi_{\text{d}}), 0.09 + 0.1 \sin(w_p t + \varphi_{\text{d}})]^\top$, $\eta_{\text{d}}(t) = [0.15 \sin(w_\phi t + \varphi_{\text{d}}), 0.15 \sin(w_\theta t + \varphi_{\text{d}}), 0.15 \sin(w_\psi t + \varphi_{\text{d}})]^\top$ (in meters and rad, respectively), where $\varphi_{\text{d}} = \frac{\pi}{6}$, $w_p = w_\phi = w_\psi = 1$, $w_\theta = 0.5$, and $\eta_{\text{d}}(t)$ is transformed to the respective $R_{\text{d}}(t)$. The gains are set as $K_{p_1} = 15$, $k_{p_2} = 75$, and $K_d = 40 I_6$.

The results are given in Figs. 3 and 4 for 15 s. Fig. 3 depicts the pose and velocity errors $e_p(t)$, $e_O(t)$, $e_v(t)$, which converge to zero for both choices of G^*, as expected. The norms of the control inputs $\tau_i(t)$ of the agents are shown in Fig. 4. Moreover, the norm of the internal forces, $\|h_{\text{int}}(t)\|$, computed via (20a), is shown in Fig. 5 (left). It is clear that G_2^* yields significantly larger internal forces, whereas G_1^* keeps them very close to zero, as proven in the theoretical analysis. The larger internal forces in the case of G_2^* are associated with the larger control inputs τ_i. This can be also concluded from Fig. 4; it is clear that inputs of larger magnitude occur in the case of G_2^*, which creates internal forces.

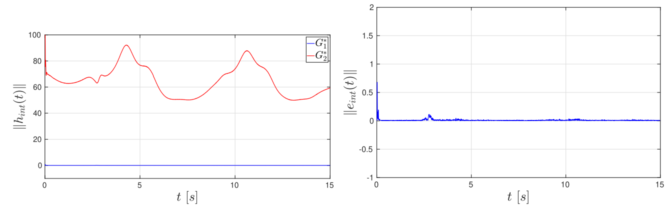

Fig. 5. Left: The signal $\|h_{\text{int}}(t)\|$ [as computed via (20a)] for the two cases of G^* and $t \in [0, 15]$ s. Right: The signal $\|e_{\text{int}}(t)\|$, when using G_1^* and for $t \in [0, 15]$ s.

Finally, we set a random force vector $h_{\text{int,d}}$ in the nullspace of G and we simulate the control law (28) with the extra component $u_{\text{int,d}} = h_{\text{int,d}}$ (see Corollary 3). Fig. 5 (right) illustrates the error norm $\|e_{\text{int}}(t)\| := \|h_{\text{int,d}}(t) - h_{\text{int}}(t)\|$, which evolves close to zero. The minor observed deviations can be attributed to model uncertainties and hence the imperfect cancelation of the respective dynamics via (28).

VIII. Conclusion

In this article, we introduce the notion of distance and bearing rigidity in SE(3) and we use the associated rigidity matrix to express the internal forces that emerge in a cooperative manipulation scheme. Based on these results, we connect the rigidity and grasp matrices via a nullspace-range relation and we provide novel results on internal-force-based cooperative manipulation control and on the relation between the interaction and internal forces. Future efforts will be directed toward using rigidity theory for object pose estimation and robust control design that minimizes the arising internal forces.

References

[1] K.-K. Oh, M.-C. Park, and H.-S. Ahn, "A survey of multi-agent formation control," *Automatica*, vol. 53, pp. 424–440, 2015.

[2] H. G. De Marina, B. Jayawardhana, and M. Cao, "Distributed rotational and translational maneuvering of rigid formations and their applications," *IEEE Trans. Robot.*, vol. 32, no. 3, pp. 684–697, Jun. 2016.

[3] X. Chen, M.-A. Belabbas, and T. Başar, "Global stabilization of triangulated formations," *SIAM J. Control Optim.*, vol. 55, no. 1, pp. 172–199, 2017.

[4] Y.-P. Tian and Q. Wang, "Global stabilization of rigid formations in the plane," *Automatica*, vol. 49, no. 5, pp. 1436–1441, 2013.

[5] S. Zhao and D. Zelazo, "Bearing rigidity theory and its applications for control and estimation of network systems: Life beyond distance rigidity," *IEEE Control Syst. Mag.*, vol. 39, no. 2, pp. 66–83, Apr. 2019.

[6] R. Tron, L. Carlone, F. Dellaert, and K. Daniilidis, "Rigid components identification and rigidity control in bearing-only localization using the graph cycle basis," in *Proc. Amer. Control Conf.*, 2015, pp. 3911–3918.

[7] H.-C. Lin, J. Smith, K. K. Babarahmati, N. Dehio, and M. Mistry, "A projected inverse dynamics approach for multi-arm cartesian impedance control," in *Proc. Int. Conf. Robot. Autom.*, 2018, pp. 1–5.

[8] F. Aghili, "A unified approach for inverse and direct dynamics of constrained multibody systems based on linear projection operator: Applications to control and simulation," *IEEE Trans. Robot.*, vol. 21, no. 5, pp. 834–849, Oct. 2005.

[9] S. Erhart and S. Hirche, "Internal force analysis and load distribution for cooperative multi-robot manipulation," *IEEE Trans. Robot.*, vol. 31, no. 5, pp. 1238–1243, Oct. 2015.
[10] F. Udwadia and R. E. Kalaba, "A new perspective on constrained motion," *Proc. Roy. Soc. A: Math., Phys. Eng. Sci.*, vol. 439, pp. 407–410, 1992.
[11] R. E. Kalaba and F. Udwadia, "Equations of motion for nonholonomic, constrained dynamical systems via Gauss's principle," *ASME J. Appl. Mech.*, vol. 60, no. 3, pp. 662–668, 1993.
[12] P. Donner, S. Endo, and M. Buss, "Physically plausible wrench decomposition for multieffector object manipulation," *IEEE Trans. Robot.*, vol. 34, no. 4, pp. 1053–1067, Aug. 2018.
[13] O. Khatib, K. Yokoi, K. Chang, D. Ruspini, R. Holmberg, and A. Casal, "Decentralized cooperation between multiple manipulators," in *Proc. 5th IEEE Int. Workshop Robot Hum. Commun.*, 1996, pp. 183–188.
[14] F. Ficuciello, A. Romano, L. Villani, and B. Siciliano, "Cartesian impedance control of redundant manipulators for human–robot co-manipulation," in *Proc. IEEE/RSJ Int. Conf. Intell. Robots Syst.*, 2014, pp. 2120–2125.
[15] T. Yoshikawa and X.-Z. Zheng, "Coordinated dynamic hybrid position/force control for multiple robot manipulators handling one constrained object," *Int. J. Robot. Res.*, vol. 12, no. 3, pp. 219–230, 1993.
[16] S. Erhart, D. Sieber, and S. Hirche, "An impedance-based control architecture for multi-robot cooperative dual-arm mobile manipulation," in *Proc. IEEE/RSJ Int. Conf. Intell. Robots Syst.*, 2013, pp. 315–322.
[17] A. Tsiamis, C. K. Verginis, C. P. Bechlioulis, and K. J. Kyriakopoulos, "Cooperative manipulation exploiting only implicit communication," in *Proc. Int. Conf. Intell. Robots Syst.*, 2015, pp. 864–869.
[18] D. Heck, D. Kostić, A. Denasi, and H. Nijmeijer, "Internal and external force-based impedance control for cooperative manipulation," in *Proc. IEEE Eur. Control Conf.*, 2013, pp. 2299–2304.
[19] C. K. Verginis, M. Mastellaro, and D. V. Dimarogonas, "Robust cooperative manipulation without force/torque measurements: Control design and experiments," *IEEE Trans. Control Syst. Technol.*, vol. 28, no. 3, pp. 713–729, May 2019.
[20] S. Erhart and S. Hirche, "Adaptive force/velocity control for multi-robot cooperative manipulation under uncertain kinematic parameters," in *Proc. Int. Conf. Intell. Robots Syst.*, 2013, pp. 307–314.
[21] A.-N. Ponce-Hinestroza, J.-A. Castro-Castro, H.-I. Guerrero-Reyes, V. Parra-Vega, and E. Olguỳn-Dỳaz, "Cooperative redundant omnidirectional mobile manipulators: Model-free decentralized integral sliding modes and passive velocity fields," in *Proc. Int. Conf. Robot. Automat.*, 2016, pp. 2375–2380.
[22] A. Marino, "Distributed adaptive control of networked cooperative mobile manipulators," *IEEE Trans. Control Syst. Technol.*, vol. 26, no. 5, pp. 1646–1660, Sep. 2018.
[23] I. D. Walker, R. A. Freeman, and S. I. Marcus, "Analysis of motion and internal loading of objects grasped by multiple cooperating manipulators," *Int. J. Robot. Res.*, vol. 10, no. 4, pp. 396–409, 1991.
[24] D. Williams and O. Khatib, "The virtual linkage: A model for internal forces in multi-grasp manipulation," in *Proc. Int. Conf. Robot. Automat.*, 1993, vol. 1, pp. 1025–1030.
[25] J. H. Chung, B. J. Yi, and W. K. Kim, "Analysis of internal loading at multiple robotic systems," *J. Mech. Sci. Technol.*, vol. 19, no. 8, pp. 1554–1567, 2005.
[26] S. Erhart and S. Hirche, "Model and analysis of the interaction dynamics in cooperative manipulation tasks," *IEEE Trans. Robot.*, vol. 32, no. 3, pp. 672–683, Jun. 2016.
[27] S. Briot and P. R. Giordano, "Physical interpretation of rigidity for bearing formations: Application to mobility and singularity analyses," *J. Mechan. Robot.*, vol. 11, no. 3, 2019, Art. no. 031006.
[28] C. K. Verginis and D. V. Dimarogonas, "Energy-optimal cooperative manipulation via provable internal-force regulation," in *Proc. IEEE Int. Conf. Robot. Automat.*, 2020, pp. 9859–9865.
[29] A. Albert, *Regression and the Moore–Penrose Pseudoinverse*. Mathematics in Science and Engineering, vol. 94, 1972, pp. 1–180. [Online]. Available: https://www.sciencedirect.com/bookseries/mathematics-in-science-and-engineering/vol/94/suppl/C
[30] B. Siciliano, L. Sciavicco, L. Villani, and G. Oriolo, *Robotics: Modelling, Planning and Control*. Berlin, Germany: Springer, 2010.
[31] L. Asimow and B. Roth, "The rigidity of graphs," *Trans. Amer. Math. Soc.*, vol. 245, pp. 279–289, 1978.
[32] G. Michieletto, A. Cenedese, and A. Franchi, "Bearing rigidity theory in se(3)," in *Proc. Conf. Decis. Control*, 2016, pp. 5950–5955.
[33] G. Michieletto, D. Zelazo, and A. Cenedese, "A unified dissertation on bearing rigidity theory," *IEEE Trans. Control Netw. Syst.*, vol. 8, no. 4, pp. 1624–1636, Dec. 2021.
[34] S. Boyd and L. Vandenberghe, *Convex Optimization*. Cambridge, U.K.: Cambridge Univ. Press, 2004.
[35] N. I. Gould, "On practical conditions for the existence and uniqueness of solutions to the general equality quadratic programming problem," *Math. Program.*, vol. 32, no. 1, pp. 90–99, 1985.
[36] T. Lee, M. Leok, and N. H. McClamroch, "Control of complex maneuvers for a quadrotor UAV using geometric methods on SE(3)," 2010, *arXiv:1003.2005*.
[37] S. P. Bhat and D. S. Bernstein, "A topological obstruction to continuous global stabilization of rotational motion and the unwinding phenomenon," *Syst. Control Lett.*, vol. 39, no. 1, pp. 63–70, 2000.
[38] H. K. Khalil, *Nonlinear Systems*, 3rd ed., Upper Saddle River, NJ, USA: Prentice-Hall, 2002, [Online]. Available: https://cds.cern.ch/record/1173048
[39] E. Rohmer, S. P. Singh, and M. Freese, "V-REP: A versatile and scalable robot simulation framework," in *Proc. IEEE/RSJ Int. Conf. Intell. Robots Syst.*, 2013, pp. 1321–1326.

Christos K. Verginis (Member, IEEE) received the Diploma in electrical and computer engineering and the M.Sc. degree in automatic control systems and robotics from the National Technical University of Athens (NTUA), Athens, Greece, in 2013 and 2015, respectively, and the Ph.D. degree in electrical engineering from the KTH Royal Institute of Technology, Stockholm, Sweden, in 2020.

He is currently an Assistant Professor in intelligent systems with Uppsala University, Uppsala, Sweden. He was a Postdoctoral Researcher with the University of Texas at Austin. He has authored more than 40 papers in scientific journals and conference proceedings. His research interests include nonlinear and adaptive control, hybrid and safety-critical systems, multi-robot systems, data-driven control, and reinforcement learning.

Dr. Verginis has received the EECI Ph.D. Award on Control for Complex and Heterogeneous Systems, 2020.

Daniel Zelazo (Senior Member, IEEE) received the B.Sc. and M.Eng. degrees in electrical engineering and computer science from the Massachusetts Institute of Technology, Cambridge, U.K., in 1999 and 2001, respectively, and the Ph.D. degree in aeronautics and astronautics from the University of Washington, Seattle, WA, USA, in 2009.

He is an Associate Professor of aerospace engineering with the Technion-Israel Institute of Technology, Haifa, Israel. He was a Research Engineer for two years with Texas Instruments, Japan, where he worked on audio compression algorithms. From 2010 to 2012, he was a Postdoctoral Research Associate and Lecturer with the Institute for Systems Theory and Automatic Control, University of Stuttgart, Stuttgart, Germany. His research interests include topics related to multiagent systems.

Dr. Zelazo is an Associate Editor of *IEEE Control Systems Letters* and Subject Editor for the *International Journal of Robust and Nonlinear Control*.

Dimos V. Dimarogonas (Senior Member, IEEE) was born in Athens, Greece, in 1978. He received the Diploma in electrical and computer engineering and the Ph.D. degree in mechanical engineering from the National Technical University of Athens (NTUA), Athens, Greece, in 2001 and 2007, respectively.

He is currently a Professor with the Division of Decision and Control, KTH Royal Institute of Technology, Stockholm, Sweden. His research interests include multiagent systems, hybrid systems and control, robot navigation, and networked control.

Dr. Dimarogonas is on the Editorial Board of *Automatica* and IEEE TRANSACTIONS ON CONTROL OF NETWORK SYSTEMS and *Unmanned Systems*. He is a senior member of the Technical Chamber of Greece.